lubricants

Technical Note

The Prediction of Wear Depth Based on Machine Learning Algorithms

Chenrui Zhu, Lei Jin, Weidong Li, Sheng Han * and Jincan Yan *

School of Chemical and Environmental Engineering, Shanghai Institute of Technology, Shanghai 201418, China; 216062153@mail.sit.edu.cn (C.Z.); 216062113@mail.sit.edu.cn (L.J.); 216062117@mail.sit.edu.cn (W.L.)
* Correspondence: hansheng654321@sina.com (S.H.); jcyan@sit.edu.cn (J.Y.)

Abstract: In this work, ball-on-disk wear experiments were carried out on different wear parameters such as sliding speed, sliding distance, normal load, temperature, and oil film thickness. In total, 81 different sets of wear depth data were obtained. Four different machine learning (ML) algorithms, namely Random Forest (RF), K-neighborhood (KNN), Extreme Gradient Boosting (XGB), and Support Vector Machine (SVM) were applied to predict wear depth. By analyzing the performance of several ML algorithms, it is demonstrated that ball bearing wear depth can be estimated by ML models by inputting different parameter variables. A comparative analysis of the performance of the different models revealed that XGB was more accurate than the other ML models at anticipating wear depth. Further analysis of the attribute of feature importance and correlation heatmap of the Pearson correlation reveals that each input feature has an effect on wear.

Keywords: ML; wear depth prediction; XGB; RF; SVM; KNN

Citation: Zhu, C.; Jin, L.; Li, W.; Han, S.; Yan, J. The Prediction of Wear Depth Based on Machine Learning Algorithms. *Lubricants* **2024**, *12*, 34. https://doi.org/10.3390/lubricants12020034

Received: 17 November 2023
Revised: 23 January 2024
Accepted: 23 January 2024
Published: 26 January 2024

1. Introduction

Rolling ball bearings are vital accessories for various types of machinery and equipment. They play a crucial role in mechanical equipment in terms of bearing force and power transmission. Due to their high rotational accuracy, high load-bearing capacity, and reliable operation, rolling ball bearings are widely used in the field of mechanical engineering equipment. An important constraint for these ball bearings is that mechanical wear becomes more severe at high temperatures, heavy loads, and high speeds [1].

Different parameter variables of the material have been proposed in order to estimate wear values based on the material. It is reported that many studies on the wear of ball bearings are based on a single parameter variable. Use a quasi-dynamic method to evaluate the characteristics of ball bearings. Based on the mathematical model, it was found that the bearing wear life reduced with the increase of axial load [2]. For the wear of angular contact ball bearings for different speed and load conditions, it was found that an increase in speed and load leads to an increase in the wear of ball bearings [3]. The Archard model in differential form is based on the Archard theory of adhesive wear and it was found that the wear value is a function of both speed and load [4]. It has been reported that the magnitude of the value of the friction coefficient is different at different wear distances by a ball-on-disk experiment, and then the amount of wear is also different [5]. It is shown that speed, load, and working distance are the main factors affecting wear.

Generally speaking, the working temperature of spindle bearings in various machinery and equipment can be as high as 300 °C. High temperature will lead to expansion of the bearing structure, which will further change the internal clearance and eventually change the internal load distribution and have a dramatic effect on the life and reliability of the bearings [6]. Therefore grease or lubricant will be added to achieve the effective reduction of friction. Lubricants usually form a film on the bearing contact surface to reduce metal-to-metal interaction. However, in actual operation, the film thickness can be variable due to differences in frictional heating and pressure, thus affecting the separation of the friction pairs [7]. Parameters such as temperature and base oil viscosity are important in the stages of wear compared to parameters such as load and wear coefficient by lubrication model analysis [8]. The thickness of the oil film was determined by the viscosity of the base oil [9]. It was reported that temperature is the main parameter for the operation of grease in roller bearings and that grease performance is strongly dependent on temperature. Further optimizes the proposed hydrostatic model by factoring the friction reduction effect of the lubricant film into the model, which becomes the basis for the proposed kinetic analysis, making the theoretical results more consistent with the actual situation [10]. It is shown that the lubricant film thickness parameter makes a great difference in wear. High-viscosity oil can reduce fretting wear at high velocity through oil film formation and friction torque depends on the viscosity of the grease base oil [11,12]. After research, it has been proven that there is a correlation between hm and maximum wear depth: the higher the hm for both materials, the lower the maximum wear depth. A thicker lubricant film increases the load capacity during mechanical contact and thus reduces wear [13].

The wear behavior of ball bearings in actual operating conditions is mainly related to load, speed, temperature, operating distance, and lubrication film thickness. Most studies have used only a few of the parameter variables to predict the wear behavior of bearings. More parameter variables should be considered to obtain more accurate prediction results. As a new interdisciplinary learning technique, ML approaches have greatly evolved for use in the field of simulation prediction. Although the ML approach requires a large amount of data, it can be observed from numerous studies that it is possible to use a limited data set to achieve the expected results. Numerous scholars have extended ML to predict the Fretting wear of low alloy steel [14], tools [15,16], ferroalloy coatings [17], and composite materials [18]. Currently, ML methods applied to predict the wear of ball bearings have not been found. These methods are exceptionally important in the face of time-consuming and costly experimental results.

In this work, AISI 52100 steel discs and AISI 52100 balls were selected as frictional subsets, and ball-disk point contact frictional wear experiments were achieved under the conditions of lubrication. The established wear test standard is ASTM G99-23. Up to 81 different wear depths of data were obtained. The 81 different sets of wear depth values obtained from different parameter conditions (skidding distance, skidding speed, normal load, temperature, film thickness) were learned and predicted by using different ML models (RF, KNN, SVM, XGB). At the same time, the performance differences of different ML algorithms in predicting wear depth behavior were found. The most important input parameters affecting wear were analyzed by means of feature importance and correlation heatmap of the Pearson correlation.

2. Materials and Methods

2.1. Data Acquisition

The friction and wear tests were conducted on a disc ball mill. This machine has a frame structure, and the main engine is mainly composed of a spindle drive system, a reciprocating stroke adjustment device, a temperature control system, a fully automatic test force loading mechanism, and other parts, which are uniformly installed and welded to the machine base. It mainly includes a rotating module and a reciprocating module. In this study, only the rotating module was applied. Test parameters can be set through the operating panel of the testing system, and specific wear values can be observed on it. The properties of the balls and discs are shown in Table 1. The lubricant selected for testing is PAO8, a lubricating grease with a base oil of PAO. That has better-bearing silence performance and high-temperature oxidation resistance, excellent performance in wear and life of rolling bearings [19]. The main properties of the base oil are shown in Table 2. Before the test, the AISI 52100 steel plate is polished with metallographic sandpaper, cleaned with ethanol for 30 min, and then dried in air. Its surface roughness is ensured to be 120 nanometers. Before starting the test, a layer of lubricant is applied to the surface of the AISI 52100 steel plate and the plate is fixed. No further lubricant is added during the tests. A total of 81 sets of data with different wear depths were obtained by varying four different parameter variables, which are shown in Table 3. Among them, the value of wear depth can be directly observed by the operating panel of the testing system. To discover the effect of oil film thickness on wear depth under different parameter variables, 81 sets of film thickness data at different pressures, speeds, and temperatures were performed based on the prediction of the commonly used Hamrock–Dowson (H-D) central film thickness equation [20]. Hamrock–Dowson (H-D) central film thickness equations:

$$H_{\propto} = 1.345 \cdot R_x \cdot U^{0.67} \cdot G^{0.53} \cdot W^{-0.067} \cdot C_0 \tag{1}$$

where, $H_{\propto}$ is the center film thickness(μm), R_x is the equivalent curvature radius (mm), U is the speed parameter (-), G is the geometry parameter (-), W is the load parameter (-), C_0 is the ellipticity influence (-). U, W, G, and C_0 are defined as,

$$U = \frac{\eta_0 \cdot (U_1 + U_2)}{2 \cdot R_x \cdot E^*} \tag{2}$$

$$W = \frac{2 \cdot F_N}{{R_x}^2 \cdot E^*} \tag{3}$$

$$G = 2 \cdot \alpha \cdot E^* \tag{4}$$

$$C_0 = 1 - 0.61 \cdot e^{(-0.752 \cdot (R_x/R_y)_{0.64})} \tag{5}$$

where U_1 is the ball speed (m/s), U_2 is the disc speed (m/s), $R_{x,y}$ is the equivalent curvature radius (mm), E^* is the equivalent Young modulus (Pa), F_N is the normal force (N), α is the pressure-viscosity coefficient (Pa^{-1}).

Table 1. Ball and disk data.

	Ball	Disc
Elastic modulus—E (GPa)	210	208
Poison coefficient—v (/)	0.29	0.283
Radius—(mm)	6.35	80
Hardness—HRC	63	60

Table 2. Lubricant properties.

Lubricant	Viscosity at 40 °C (mm^2/s)	Viscosity at 100 °C (mm^2/s)	Viscosity Index	Specific Gravity (g/cm^3)
PAO8	50.72	8.34	138	0.8326

Table 3. Wear test parameters.

Descriptions	Value
Normal Load (N)	20, 30, 50
Sliding speed (mm/s)	200, 500, 800
Sliding distance (m)	250, 500, 750
Motion	Rotating
Temperature (°C)	20, 60, 100

2.2. ML Algorithms

Data-driven ML analysis provides novel insights analyzing the wear amount, which are often unattainable with traditional analysis. Machine learning algorithms have been used for wear loss testing in different studies before. Therefore, in this study, supervised ML was used for regression analysis to discover the correlation between input parameters (normal load, sliding speed, temperature, lubricating film, sliding distance) and output parameters (wear depth). The ML algorithm trained four different models: RF, KNN, XGB, and SVM. The purpose of selecting different models is to determine the most suitable model by comparing the prediction accuracy of different models. Ball-on-disk wear data were used to identify relationships between input and output parameters and to forecast wear behavior. The workflow of the ML applied in the present work is revealed in Figure 1. A brief description of the ML algorithms used in this study is presented below.

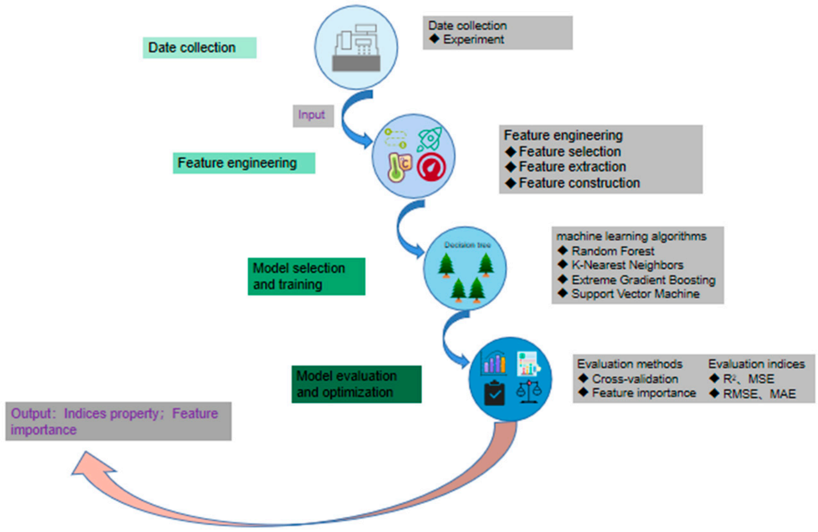

Figure 1. ML workflow diagram.

The RF model was formally defined by Breiman in 2001 [21], and the RF algorithm is a supervised learning algorithm containing multiple decision trees. Decision trees are used to learn and develop from training examples. RF is applied to both classification and regression problems. In regression problems, the average of the predictions of the entire decision tree is calculated for given test data in the random forest. It can be used for the final prediction of the random forest. Repeated sampling is a valuable method in statistics for reducing the variance of estimates. By repeated sampling, the mean square error of random forest prediction and the probability of overfitting are less than those of a single decision tree. Due to this unique property, RF is usually superior to most other ML algorithms.

The KNN model is a frequently used supervised learning method that is convenient and fast for small amounts of data and easy to visualize. The principle can be described as that the nearest K samples in the training set are found based on a specified distance measure and predictions are made based on information from these K "neighbors". The complexity of the KNN model can be determined depending on the value of K. A smaller value of K is susceptible to outliers, and conversely, a larger value of K is susceptible to sample balance problems. Therefore, the appropriate K value needs to be selected for performance optimization based on the type of data and complexity of the problem. Another special consideration for KNN models is the assignment of uniformity or distance-based weights to neighboring points [22].

The XGB model consists of multiple decision trees and is an improvement on the traditional gradient-boosted decision tree. The complexity of the tree is taken into account for XGB and fewer iterations are required to achieve the same training result, and then the speed of operation is greatly increased. XGB extends the loss function by a second-order Taylor series expansion to allow the model to converge quickly. It also adds a regularization term to the loss function to prevent overfitting. In the XGB model, the residuals of the true value predicted by each decision tree and the sum of the predictions of all the previous decision trees are then summed up to give the final result. It has attracted the interest of many researchers in the field due to its advantages in speed and accuracy [23].

The SVM model is a common ML method used in supervised learning, which was introduced in 1995 by Corinna et al. [24]. In addition to linear and non-linear classification, SVM models are capable of resolving regression problems as well as anomaly detection tasks. It is possible to divide different classes of samples by finding a hyperplane, and then the samples are divided in accordance with the maximum interval principle indicating the most effective generalization ability. SVM can effectively perform nonlinear classification using kernel functions, which map the implicit input into a high-dimensional feature space. There are several different variants of the SVM algorithm depending on the kernel function [25].

RF is constructed by a regression algorithm that calculates the average of the predictions of all decision trees in a random forest. It uses this as the final prediction. KNN makes predictions are based on feature similarity by calculating the distance (Euclidean distance) between the test samples and the samples in the training set. XGB is based on regression trees that add up the predictions of each regression tree for each sample as the final prediction. The SVM is based on a hyperplane that divides the samples into different categories and fits the model with the maximum number of data points.

2.3. Parameter Optimization of ML Models

Overfitting is a potential concern when developing machine learning models, where training errors may decrease while testing errors increase rapidly. To address this issue, the objective function of the model was optimized. Due to the fact that the XBG model itself can optimize the objective function, the main focus is on optimizing the objective function settings for RF, KNN, and SVM models. The main method used is the least squares method. Model analysis mainly uses linear regression analysis, and the least squares method can estimate the most suitable line, minimizing the error between actual data and line estimation and improving the efficiency of the model [17].

2.4. Evaluation Parameters

In this study, four different metrics of coefficient of determination (R^2), the mean square error (*MSE*), the root mean square error (*RMSE*), and the mean absolute error (*MAE*) were used to measure the performance of ML models [18]. Each of these performance indicators provides basic information about the performance of the model used from a different perspective.

$$R^2 = \frac{\sum_{i=1}^{n} \left(y_i - \hat{y}_i\right)^2}{\sum_{i=1}^{n} \left(y_i - \overline{y}_i\right)^2} \tag{6}$$

$$MSE = \frac{1}{n}\sum_{i=1}^{n}(y_i - \hat{y}_i)^2 \tag{7}$$

$$RMSE = \sqrt{\frac{\sum_{i=1}^{n} \left(y_i - \hat{y}_i\right)^2}{n}} \tag{8}$$

$$MAE = \frac{1}{n}\sum_{i=1}^{n} |y_i - \hat{y}_i| \tag{9}$$

where n is the number of trials, y_i denotes the true measured output value, $\hat{y}_i$ denotes the predicting

Output values and $\bar{y}$ is the average of the actual measured values.

3. Results and Discussion

The aim of this work is to predict the wear loss behavior of ball bearings by means of ML. Four ML algorithms of RF, KNN, XGB, and SVM have been applied to predict the wear depth by five input parameters: sliding distance, sliding speed, normal load, temperature, and film thickness of the oil. Wear depth was taken as the output for wear loss in the algorithms. To ensure the accuracy of the ML model, 81 sets of data collected in the laboratory were divided into 75% for the training set and 25% for the validation set [26]. The training set is used to train the model to optimize parameters related to input and output, while the test set is used to evaluate the performance of the model by comparing its results with various ML algorithms mentioned in the following section of this study. The ML algorithm contains 60 and 21 data points (a total of 81 data points) in the training and validation sets, respectively, for wear depth. This method uses a k-value of 5 and all data are provided as test and training data for the k-fold cross-validation. Four different evaluation criteria such as R^2, *MSE*, *RMSE*, and *MAE* were employed [27].

3.1. Model Performance Evaluation

As shown in Figure 2, there is a certain relationship between input parameters and output target parameters during wear. It can be observed that the sliding distance, sliding speed, normal load, temperature, and oil film thickness all have a non-linear relationship with the wear depth of the output variable. Due to the complex behavior of nonlinear systems or functions, their output data cannot be simply determined by input data. It has been further confirmed that the wear behavior of bearings is caused by a combination of multiple factors. Predicting the relationship between multiple input features and output features is more in line with the ideas of machine learning.

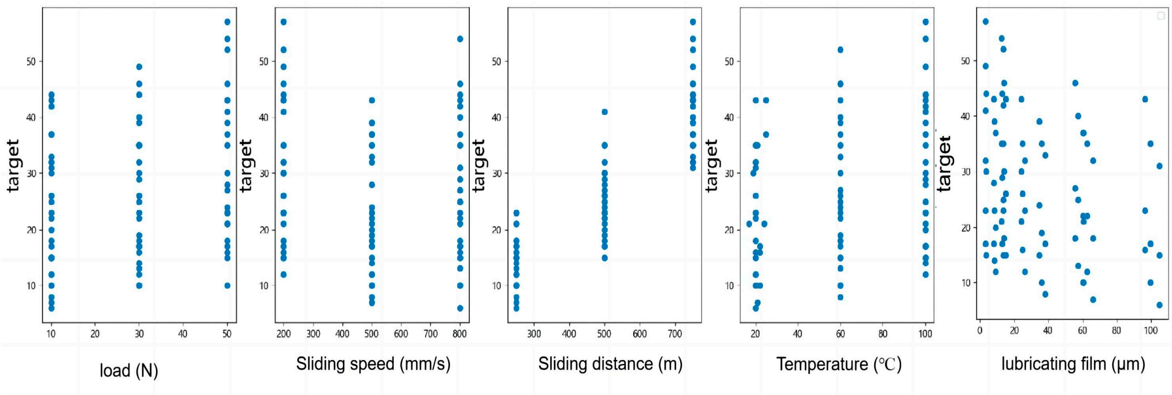

Figure 2. Pairwise relationship between different inputs and target outputs.

The error cumulative frequency chart shown in Figure 3 can provide a more comprehensive evaluation of the predictive accuracy and stability of the model. By viewing the curves in the graph, we can understand the performance of the model within different error ranges. The absolute error range of models RF, KNN, and XGB is smaller than that of model SVM, and the cumulative frequency is higher, indicating that models RF, KNN, and XGB have higher prediction accuracy and stability.

As depicted in Equation (2), a model with no error yields an R^2 value of 1. When R^2 falls within the range of 0.6 to 0.9, it indicates satisfactory performance of the model. Conversely, if R^2 is below 0.5, the model exhibits poor predictive capability. Compared to other evaluation criteria, R^2 provides a more accurate reflection of the model's precision due to its correlation with RMSE and MSE, which measure squared errors between actual and predicted outputs. Additionally, MAE robustly captures the average absolute difference between measured and true values in both predicted and actual outputs while being less affected by outliers [28].

The ML wear depth prediction model with performance indicators is shown in Table 4. The R^2 attribute of the validation set ranges from 0.29 to 0.88 by using the four ML models. The ML models with different M-values are between 2.95 and 7.29, the mean square error is between 14.48 and 87.2, and the RMSE is between 3.62 and 8.81. The lowest R^2 value is generated by SVM, and the highest R^2 value is generated by XGB. These statistical performances indicate that the results provided by SVM and KNN are not very accurate. The other two models, RF and XGB, can give satisfactory results based on input parameters when predicting wear depth. XGB produces the maximum generated R^2 of 0.88 compared with other models. It is shown that XGB accurately predicts the wear depth from the input parameters, with a prediction accuracy of 88%. The root means square error (*MSE*), root mean square error (*RMSE*), and absolute error (*MAE*) of the model are 14.48, 3.62, and 2.95, respectively. The performance of the decision tree-based RF model is also satisfactory, with an R^2 value of 0.84, almost identical to the performance of XGB. However, it is found that the tree-based ML model (RF, XGB) produces more accurate predictions than the multi-level model (SVM), which has a very low R^2 value of only 0.29. One possible explanation may be that the dataset is relatively small with a low dimension. Therefore, it may be that insufficient data and insufficient induction capacity lead to overfitting problems.

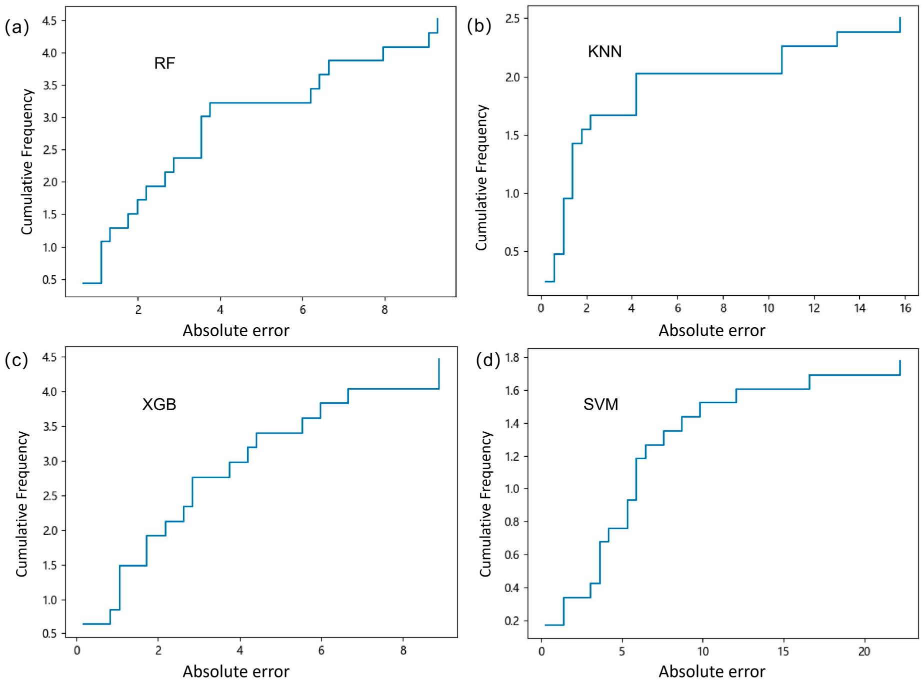

Figure 3. Accumulated frequency chart of errors.

Table 4. Model property in predicting wear depth.

ML Model	*MAE*	*RMSE*	*MSE*	R^2
KNN	4.54	5.69	38.41	0.68
RF	3.25	4.14	18.3	0.84
SVM	7.29	8.81	87.2	0.29
XGBoost	2.95	3.62	14.48	0.88

3.2. Comparison between Experimental and Predicted Values

The predicted and experimental values of the constructed models are shown in Figure 4. It can be seen that the prediction performed by RF (a), KNN (b), and XGB (c) models are close to the experimental values, which is acceptable. A large deviation in the prediction results and a very low level of prediction accuracy can be found when the prediction was performed by the SVM (d) model. The reason for this result is that SVM requires a larger dataset and higher dimensionality compared to other models, so it may be due to overfitting issues caused by insufficient data and generalization ability.

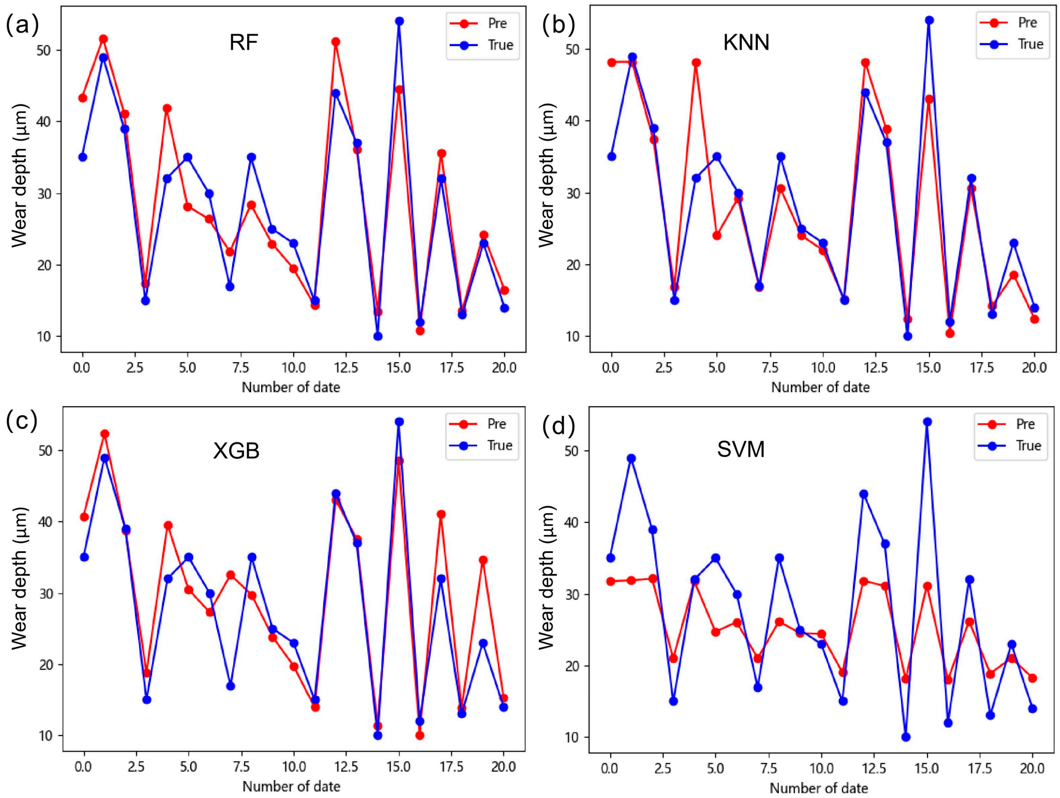

Figure 4. Experimental and predicted wear losses: (**a**) RF results, (**b**) KNN results, (**c**) XGB results and (**d**) SVM results.

3.3. Regression Analysis of Model Results

A graphical analysis of the regression results for all models is shown in Figure 5. It can be clearly seen that wear depth can be predicted by RF (a), XGB (c), and KNN (b) satisfactorily, as essentially all data points are distributed around the line of best fit. XGB (c) has the most accurate prediction with an R^2 value of 0.88. SVM (d) did not perform very well on the verification dataset, and the margin of error of SVM was significantly larger than that of XGB, RF, and KNN. The Taylor diagram comparing the models can be seen in Figure 6. And it can be found that the correlation coefficients of the models are all very high, indicating that these models have good simulation effects.

3.4. The Influence of Different Characteristic Parameters on Wear Amount

Feature importance refers to a technique for assigning scores to input features in predictive modeling. It is performed by representing the relative importance of each feature in making a prediction [21]. By feature importance analysis, it is possible to investigate which intrinsic properties determine the wear depth. "Feature importance" for XGB models indicates the usefulness and the value of each feature in building the augmented decision tree in the model. It can be explained that the feature has an unusual magnitude in output prediction. A plot of the feature value for the forecast of ball bearing wear depth based on XGB is shown in Figure 7. It can be seen that all the input features scored, indicating that they all play a role in prediction. Among all the features, sliding distance scored the highest, indicating that sliding distance was the most dominant feature. This may be due to the fact that the metal on the contact surface becomes softer with a longer sliding distance, and thus wear increases. Oil film thickness was identified as the second most important feature for predicting wear depth. This indicates that bearing wear is largely dependent on the ability of the lubricating oil film to separate the rolling elements, as the film thickness determines the load shared between the metal contact surface and the lubricant. In the other input parameters, temperature, sliding speed, and load on the output parameters of the wear depth prediction have a certain influence. Figure 8 shows the correlation heatmap of the Pearson correlation coefficient matrix of the five features for wear depth prediction [29]. It shows that the top three features that have the highest correlation coefficients are sliding distance, lubricating film, and temperature, consistent with the feature importance analysis as shown in Figure 7.

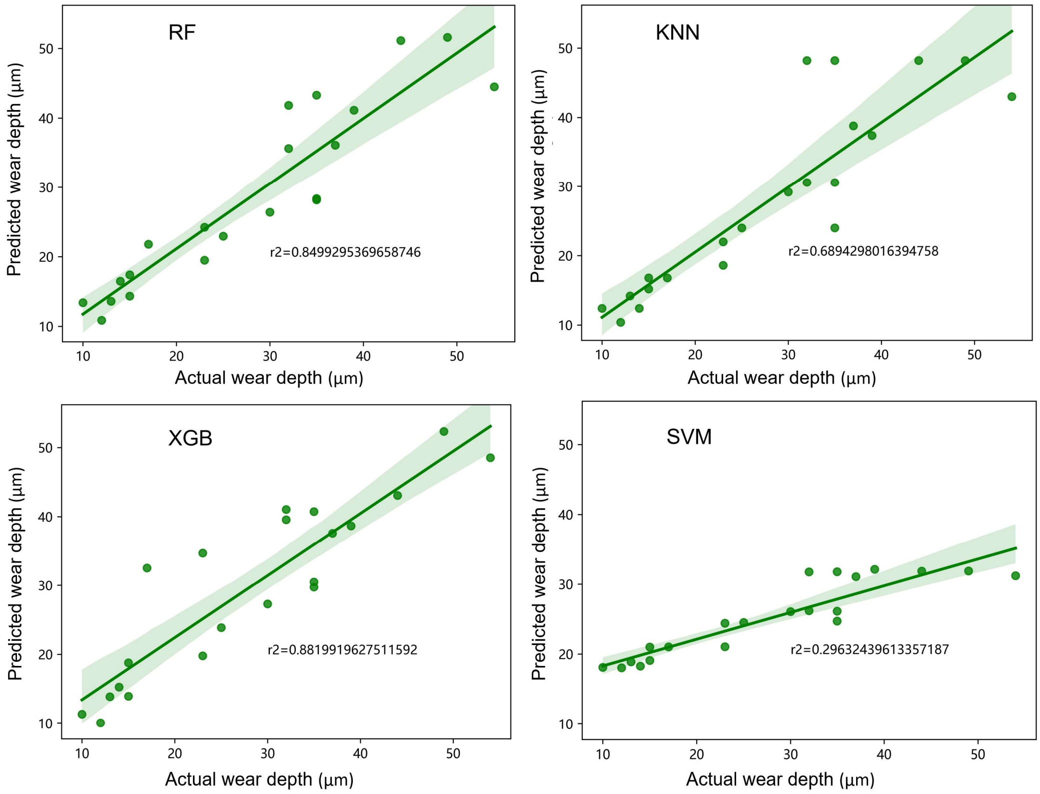

Figure 5. Regression analysis diagram of model results.

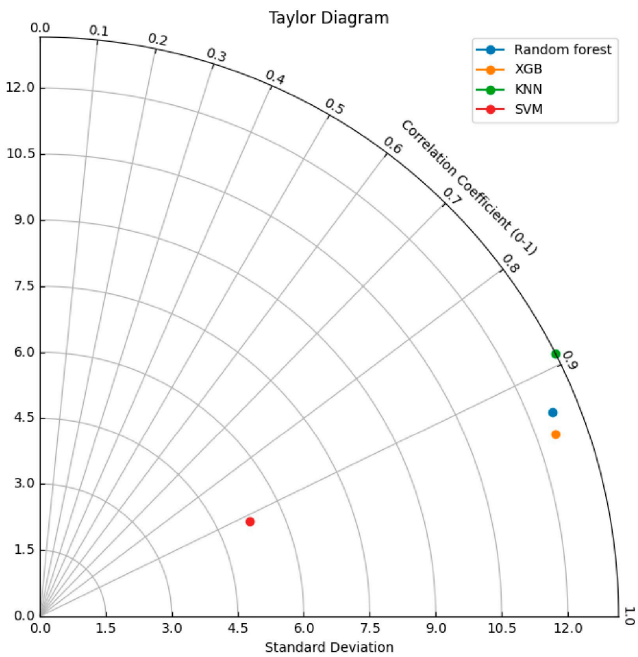

Figure 6. Plot of results in Taylor diagram.

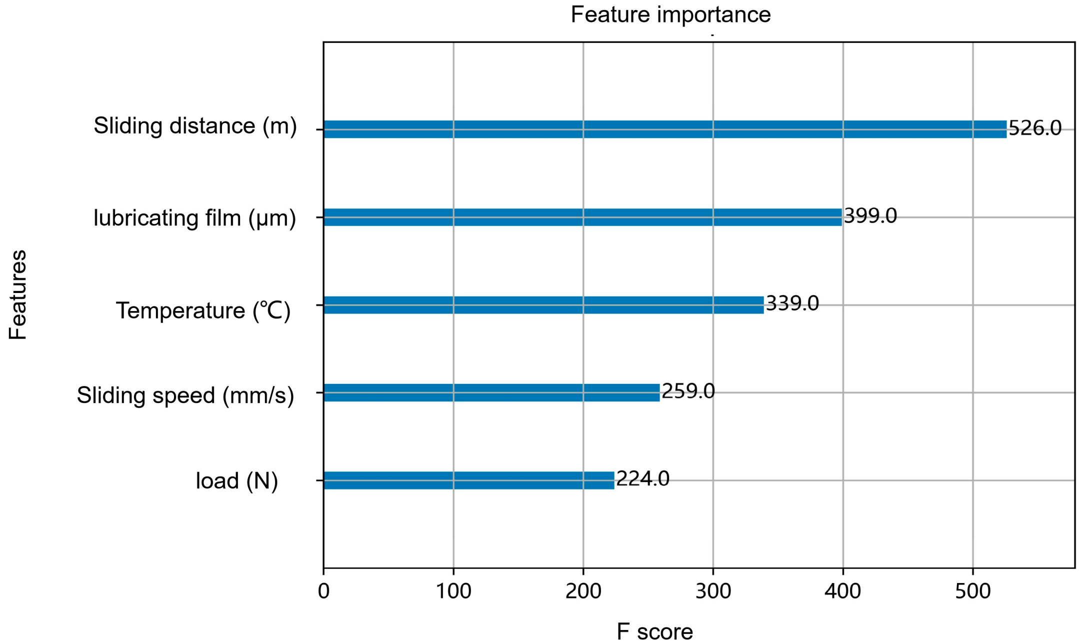

Figure 7. Feature importance for predicting wear depth.

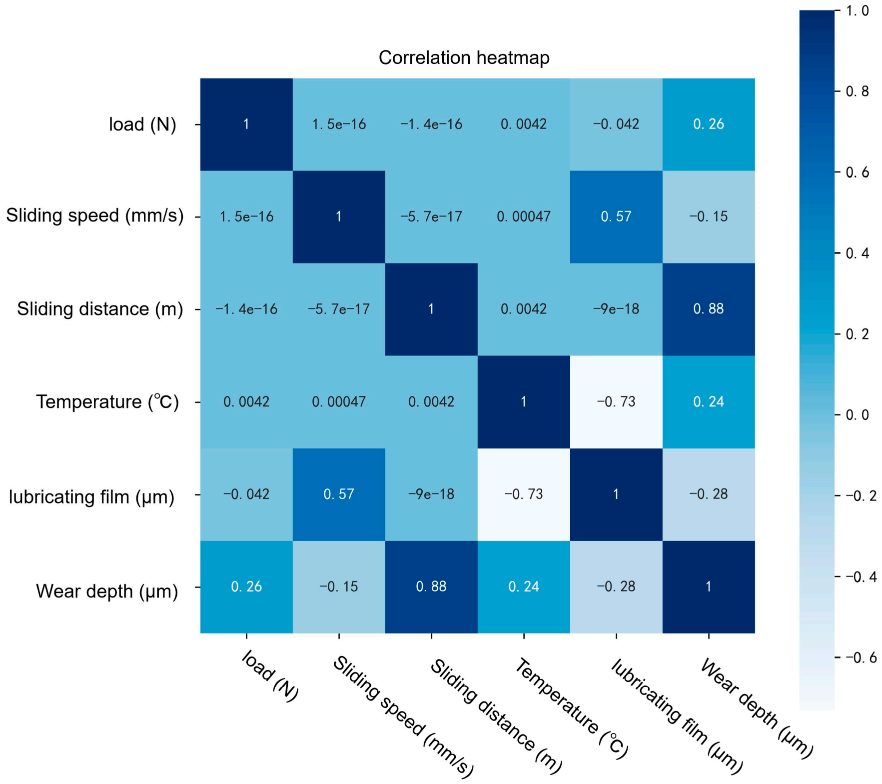

Figure 8. The heatmap of Pearson correlation coefficient matrix of the five features for wear depth.

The results show that both XGB and RF can predict ball bearing wear depth well according to different input variables. While ensuring personal safety and the normal operation of mechanical equipment, it can also reduce a certain burden on the time and cost of the designer. Through the attribute analysis of the importance of features and correlation heatmap of the Pearson correlation, the influence of different working parameters on wear behavior can be understood more deeply.

4. Conclusions

A total of 81 different sets of disc wear depth values were obtained from the experiment by varying different operational parameters. Four different ML algorithms were trained to predict wear depths. It is found that the wear depth values of the ball bearings can be predicted by the ML models accurately. With the proposed model, time loss, production costs, and man-hours could be saved.

Discovering paired relationships between different inputs and target outputs: the sliding distance, sliding speed, normal load, temperature, and oil film thickness all have a non-linear relationship with the wear depth of the output variable. It has been further confirmed that the wear behavior of bearings is caused by a combination of multiple factors.

XGB outperformed the other ML models in terms of prediction (R^2 = 0.88, MSE = 14.48, $RMSE$ = 3.62, MAE = 2.95). When predicting wear, the algorithm produced the best results among the proposed machine learning algorithms. Further demonstrating through Taylor plots that the XGB model has high accuracy.

These characteristics are important for estimating flank wear with a given set of machine parameters and experimental trials. Further analysis of the attribute of feature importance and correlation heatmap of the Pearson correlation reveals that each input feature has an effect on wear. It is shown in the results that the wear depth is most affected by sliding distance, oil film thickness, and temperature.

Overall, the current work provides a fast and reliable method for predicting the depth of bearing wear. Such findings from ML analysis can be used in material wear analysis for specialized tribological applications.

Author Contributions: Conceptualization and Writing—original draft: C.Z.; Methodology: W.L.; Formal analysis and investigation: L.J.; Writing—review and editing: J.Y.; Supervision: S.H. All authors contributed to reviewing and editing the manuscript. All authors have read and agreed to the published version of the manuscript.

Funding: This work was supported by the National Natural Science Foundation of China [Project Number 22075183, 22008155, 22278269 and 21975161], Industrial Collaborative Innovation Project of Shanghai [Project Number 2021-cyxt1-kj37 and XTCX-KJ-2022-70], Leading Talents Program of Shanghai [Project Number 053], Natural Science Foundation Project of Shanghai [Project Number 22ZR1426100], Foundation of Science and Technology Commission of Shanghai Municipality [22010503900], Guangdong Basic and Applied Basic Research Foundation [2020A1515011102], Project of Department of Education of Guangdong Province [2018KTSCX219].

Data Availability Statement: The data that support the findings of this study are available on request from the corresponding author. The data are not publicly available due to privacy or ethical restrictions.

Conflicts of Interest: The authors declare no conflicts of interest.

References

1. Jiang, S.X.; Qun, L.X.; Yan, F.; Yi, Q.Z. Tribo-dynamic analysis for aero ball bearing with 3D measured surface roughness. *Eng. Fail. Anal.* **2022**, *131*, 105848.
2. Yu, G.W.; Xia, W.; Song, Z.Y.; Wu, R.; Wang, S.; Yao, Y. Wear-life analysis of deep groove ball bearings based on Archard wear theory. *J. Mech. Sci.* **2018**, *32*, 3329–3336. [CrossRef]
3. Fu, X.Y.; Wei, L.; Zhang, Y.; Li, S. Comparative study of bearing wear in spindle system at different working conditions. *Mech. Based Des. Struct. Mech.* **2023**, *51*, 6184–6203. [CrossRef]
4. Xue, Y.; Chen, J.; Guo, S.; Meng, Q.L.; Luo, J. Finite element simulation and experimental test of the wear behavior for self-lubricating spherical plain bearings. *Friction* **2018**, *6*, 297–306. [CrossRef]
5. Shu, Y.J.; Shen, F.; Ke, L.L.; Wang, Y.S. Adaptive finite element simulation and experimental verification for f-retting wear of PVDF piezoelectric thin films. *Wear* **2022**, *502–503*, 204395. [CrossRef]
6. Ricci, M.C. Internal Loading Distribution in Statically Loaded Ball Bearings Subjected to an Eccentric Thrust Load. *Math. Probl.* **2009**, *2009*, 471804. [CrossRef]
7. Mannan, A.; Pozzebon, M.L.; Daniel, W.J.T.; Meehan, P.A. Temperature Effect on Load Distribution, Friction, and Wear of a Grease-Lubricated Spherical Roller Bearing (SRB). *Tribol. Trans.* **2023**, *66*, 144–161. [CrossRef]

8. Pozzebon, M.L.; Lin, C.L.; Meehan, P.A. On the Modeling of Wear in Grease-Lubricated Spherical Roller Bea-rings. *Tribol. Trans.* **2020**, *63*, 806–819. [CrossRef]
9. Cen, H.; Lugt, P.M. Film thickness in a grease lubricated ball bearing. *Tribol. Int.* **2019**, *134*, 26–35. [CrossRef]
10. Harris, T.A.; Kotzalas, M.N. Advanced Concepts of Bearing Technology: Rolling Bearing Analysis. In *Rolling Bearing Analysis*; Routledge: London, UK, 2006.
11. Gonçalves, D.; Pinho, S.; Graça, B.; Campos, A.V.; Seabra, J.H.O. Friction torque in thrust ball bearings lubri-cated with polymer greases of different thickener content. *Tribol. Int.* **2016**, *96*, 87–96. [CrossRef]
12. Maruyama, T.; Saitoh, T.; Okouchi, A. Differences in Mechanisms for Fretting Wear Reduction between Oil and Grease Lubrication. *Tribol. Trans.* **2017**, *60*, 497–505. [CrossRef]
13. Sedlaček, M.; Podgornik, B.; Vižintin, J. Influence of surface preparation on roughness parameters, friction and wear. *Wear* **2009**, *266*, 482–487. [CrossRef]
14. Baydoun, S.; Fartas, M.; Fouvry, S. Comparison between physical and machine learning modeling to predict fretting wear volume. *Tribol. Int.* **2023**, *177*, 107936. [CrossRef]
15. Alajmi, M.S.; Almeshal, A.M. Predicting the Tool Wear of a Drilling Process Using Novel Machine Learning XGBoost-SDA. *Materials* **2020**, *13*, 4952. [CrossRef]
16. Shen, Y.; Yang, F.; Habibullah, M.S.; Ahmed, J.; Das, A.K.; Zhou, Y.; Ho, C.L. Predicting tool wear size acro-ss multi-cutting conditions using advanced machine learning techniques. *J. Intell. Manuf.* **2021**, *32*, 1753–1766. [CrossRef]
17. Altay, O.; Gurgenc, T.; Ulas, M.; Özel, C. Prediction of wear loss quantities of ferro-alloy coating using different machine learning algorithms. *Friction* **2020**, *8*, 107–114. [CrossRef]
18. Aydin, F.; Durgut, R.; Mustu, M.; Demir, B. Prediction of wear performance of ZK60 / CeO2 composites usin-g machine learning models. *Tribol. Int.* **2023**, *177*, 107945. [CrossRef]
19. Li, W.; Yang, Z.; Zha, F. Preparation of Well-Dispersed Lubricant Additives with Excellent Antiwear Ability Under High Load. *Tribol. Lett.* **2020**, *68*, 94. [CrossRef]
20. Hamrock, B.J.; Dowson, D. Isothermal Elastohydrodynamic Lubrication of Point Contacts: Part III—Fully Flood-ed Results. *J. Lubr. Technol.* **1976**, *99*, 264. [CrossRef]
21. Statistics, L.B.; Breiman, L. Random Forests. *Mach. Learn.* **2001**, *45*, 5–32.
22. Hasan, M.S.; Kordijazi, A.; Rohatgi, P.K.; Nosonovsky, M. Triboinformatic modeling of dry friction and wear of aluminum base alloys using machine learning algorithms. *Tribol. Int.* **2021**, *161*, 107065. [CrossRef]
23. Li, J.; An, X.; Li, Q.; Li, Q.; Wang, C.; Yu, H.; Zhou, X.; Geng, Y. Application of XGBoost algorithm in th-e optimization of pollutant concentration. *Atmos. Res.* **2022**, *276*, 106238. [CrossRef]
24. Cortes, C.; Vapnik, V. Support-vector networks. *Mach. Learn.* **1995**, *20*, 273–297. [CrossRef]
25. Brereton, R.G.; Lloyd, G.R. Support Vector Machines for classification and regression. *Analyst* **2010**, *135*, 230–267. [CrossRef]
26. Mustafa, U.; Osman, A.; Turan, G.; Cihan, O. Surface roughness prediction of machined aluminum alloy with w-ire electrical discharge machining by different machine learning algorithms. *J. Mater. Res. Technol.* **2020**, *9*, 12512–12524.
27. Kong, D.; Chen, Y.; Li, N. Gaussian process regression for tool wear prediction. *Mech. Syst. Signal Proc.* **2018**, *104*, 556–574. [CrossRef]
28. Matrenin, P.; Safaraliev, M.; Dmitriev, S.; Kokin, S.; Eshchanov, B.; Rusina, A. Adaptive ensemble models for medium-term forecasting of water inflow when planning electricity generation under climate change. *Energy Rep.* **2022**, *8*, 439–447. [CrossRef]
29. Zhao, L.; Biao, W. Prediction of ideal strength by machine learning. *Mater. Chem. Phys.* **2023**, *299*, 127476.